

Polymorphism in stratum corneum lipids

Boonsri Ongpipattanakul ^{a,*}, Michael L. Francoeur ^{b,1}, Russell O. Potts ^{b,2}

^a Department of Pharmaceutics, School of Pharmacy, University of Wisconsin, Madison, WI, USA

^b Pfizer Central Research, Groton, CT, USA

(Received 4 August 1993)

Abstract

Fourier transform infrared spectroscopy (FTIR) was employed to investigate the thermotropic phase behavior of stratum corneum lipid multilamellae. Stratum corneum (SC), the uppermost layer of mammalian skin, is unusual in many respects. It has been demonstrated that the lipids of the stratum corneum provide the primary electrical and transport resistance in the skin. These lipids are unusual in their composition, structure and localization; they contain only cholesterol, fatty acids and ceramides and they form broad, multi-lamellar sheets which are located extracellularly. The FTIR results from both the symmetric CH₂ stretching and the CH₂ scissoring vibrations suggest that the SC lipids exhibit polymorphic phase behavior below the main phase transition temperature. The multiple phases are most likely crystalline mixtures of different alkyl chain packings, along with solid-liquid phases. Similarities between the FTIR results reported here for SC lipids and those obtained for cholesterol-containing gel phase phospholipids suggest that the non-uniform distribution of cholesterol occurs in each system.

Key words: FTIR; Stratum corneum lipid; Lipid; Thermotropic phase behavior; Phase heterogeneity; Cholesterol

1. Introduction

It is established that stratum corneum (SC), the outer layer of mammalian epidermis, is rate-limiting to solute transport [1,2] and tissue water loss [3,4]. A major unresolved issue is the relationship between the tissue ultrastructure and its functionality. This question is often recognized as having both clinical and pharmaceutical relevance. Histologically, SC consists of keratinized, biologically inactive cells surrounded by multiple lipid lamellae, forming the only continuous phase within the SC. Composition analysis shows that the SC lipid sheets are comprised chiefly of fatty acids, ceramides, and cholesterol in the approximate mole ratio of 0.25:0.25:0.50; phospholipids found commonly in

most biological membranes are virtually absent. Furthermore, the fatty acids and ceramides are characterized by a distribution of long, saturated alkyl chains; the ceramides also contain asymmetric chain lengths [5]. Despite the complexity, electron micrographs of SC strongly support the formation of lamellar structures in these lipids [6,7].

As detailed information on the physicochemical properties of SC lipids is essential for a better understanding of the tissue function, several biophysical techniques have been employed to study SC lipids. These include X-ray diffraction [8–10], differential scanning calorimetry (DSC) [11], nuclear magnetic resonance (NMR) [12–14], and infrared (IR) [4,15] spectroscopies. In general, these results show that SC lipids are characterized by a complex chain-melting transition between about 60 and 80°C. In addition, numerous transitions of unknown origins have been observed at other temperatures [3] and complex polymorphism is common [8,9,14].

In this investigation, we have extended previous IR measurements to study chain-melting and chain-packing interactions of SC lipids in greater detail. Porcine SC, which has been shown to be equivalent to human SC in terms of tissue integrity and lipid composition,

* Corresponding author. Present address: Genentech, Inc., 460 Point San Bruno Boulevard, South San Francisco, CA 94080, USA. Fax: +1 (415) 2253191.

¹ Present address: Pharmetrix, Inc., Menlo Park, CA 94025, USA.

² Present address: Cygnus Therapeutic Systems, Redwood City, CA 94063, USA.

Abbreviations: SC, stratum corneum; DSC, differential scanning calorimetry; NMR, nuclear magnetic resonance; IR, infrared; FTIR, Fourier transform infrared; ν_s CH₂, the symmetric CH₂ stretching frequency; DPPC, dipalmitoyl-DL- α -phosphatidylcholine.

was employed throughout this study [16]. The results suggest a complex phase behavior for SC lipids where at physiological temperatures fluid and solid phases coexist. Moreover, solid-phase heterogeneity is noted at temperatures below the chain-melting transition. These results demonstrate a number of interesting similarities, from the perspective of alkyl chain vibrational spectra, between the ceramide-based SC lipids and the cholesterol-containing phospholipid bilayers.

2. Materials and methods

2.1. Porcine stratum corneum

Sheets of porcine SC were isolated according to the procedure described by Golden et al. [11]. In brief, skin from the upper thoracic area was removed immediately after the animal was sacrificed. Excessive hair was removed with clippers and the skin was dermatomed (Padgett Dermatome, Kansas City, KS) to a thickness of 500 μm . The split-thickness skin was then placed, dermal side down, on filter paper saturated with 0.5% crude trypsin (type II, Sigma Chemical Co., St. Louis, MO). After incubation at room temperature for 6 h, the SC was peeled away from the underlying tissue. The resultant sample was then gently rinsed with distilled water to remove any adherent epidermal cells, and air dried before storing in a desiccator.

2.2. Extracted lipids and delipidized stratum corneum

Lipids were isolated from porcine SC following the method of Wertz and Downing [17]. The SC was first rinsed with cold hexane to remove surface lipids. Samples were then incubated for 2 h in each of three successive extraction mixtures of chloroform: methanol (2:1, 1:1, 1:2; v/v) followed by an overnight extraction in pure methanol. All solvent fractions were combined and evaporated to dryness under a nitrogen atmosphere. Trace amount of solvent was removed by placing the sample in a vacuum until a constant weight was attained. The isolated lipids were then stored at -20°C under a nitrogen atmosphere until used. Samples of the lipid-depleted SC were kept in a desiccator.

2.3. Lipid film from isolated porcine stratum corneum

Extracted lipids were dissolved in a small volume of chloroform/methanol (2:1; v/v). This solution was transferred to a small container and the solvent was removed by evaporation in a stream of N_2 . A lipid dispersion was prepared from this sample at a concentration of 5 mg/ml, using a procedure similar to that described by White et al. [8]. In brief, the mixture was slowly heated to 80°C while sonicated, followed by

cooling to room temperature. The mixture was cycled through heating/sonication and cooling at least three times until a homogeneous dispersion was obtained. A small aliquot (300 μl) was subsequently deposited on a ZnS infrared transparent window and equilibrated at room temperature and 75% relative humidity for at least 48 h.

2.4. Sample preparation for infrared evaluation

Each sample, either SC or lipid film, was placed between two ZnS windows. The circumference of the sample-sandwich was wrapped with electrical tape to prevent dehydration. Previous study has shown this procedure to maintain a constant moisture content (less than 10%) in SC samples [11]. The temperature was directly monitored by a alumel-chromel microthermocouple inserted into a small hole drilled into one window. The sample assembly was placed in a variable temperature holder inside the infrared spectrometer. The sample holder was connected to a Lauda circulating water bath (RC-6, Brinkmann Instruments) whose temperature was controlled using a personal computer. This computer was interfaced to the spectrometer workstation and the sample thermocouple, allowing temperature control and data acquisition. The sample was heated at approximately $10^\circ\text{C}/\text{h}$ and the temperature was maintained to within 0.2°C .

2.5. FTIR data acquisition

The sample absorbance in the mid-IR region ($400\text{--}4000\text{ cm}^{-1}$) was measured in a Nicolet FTIR spectrometer (model 730, Nicolet Instruments, Madison, WI) equipped with a mercury-cadmium-telluride detector. At each temperature studied, 200 scans were collected, co-added and Fourier transformed using a Happ-Genzel apodization function to give a spectral resolution of 2 cm^{-1} . The absorbance spectrum of each sample was obtained by ratioing the transmittance against a blank background. Data analyses were performed using software supplied with the model 730 spectrometer. Peak positions were determined by a polynomial least squares method, with an uncertainty of less than $\pm 0.1\text{ cm}^{-1}$. Second derivative spectra were obtained by the use of a Savitsky-Golay procedure. To determine the bandwidth at various peak heights, ASCII files of the data were analyzed using software provided by Douglas Moffatt (National Research Council, Ottawa, Canada). Finally, Fourier self-deconvolutions were performed using a Lorentzian line shape function and a Bessel apodization function with the appropriate half-bandwidth and resolution enhancement factor.

3. Results

The stratum corneum is a complex composite of lipids and proteins, largely compartmentalized into separate domains. While methylene group vibrations are particularly useful in studying lipid alkyl chain conformation and packing, side chains of amino acid residues in proteins can also contribute to the IR absorbance, thereby complicating spectral interpretation. Hence, in order to identify the origins of the methylene (CH_2) group vibrations, spectra of porcine SC (illustrated in Fig. 1) were compared before and after exhaustive lipid extraction with a series of chloroform/methanol solvents. The results demonstrate a dramatic reduction in the absorbance of the CH_2 stretching region ($2930\text{--}2845\text{ cm}^{-1}$) in the lipid depleted sample. Estimation of the area under the symmetric CH_2 stretching band ($2870\text{--}2830\text{ cm}^{-1}$) after a baseline correction, gave the values of 2.31 ± 0.14 and 0.15 ± 0.03 ($\pm \text{S.E.}$, $n = 3$) for the control and the lipid-extracted samples, respectively. In addition, the CH_2 scissoring region ($1480\text{--}1460\text{ cm}^{-1}$) was similarly reduced.

The peak position of the symmetric CH_2 stretching band is commonly used to monitor the thermotropic phase transition of alkyl chains in phospholipids [18]. Fig. 2 shows the temperature dependence of the symmetric CH_2 stretching frequency ($\nu_s\text{CH}_2$) for SC hydrated at 75% relative humidity. There was a gradual increase in $\nu_s\text{CH}_2$ from -10 to about 60°C , with a small, but reproducible inflection at about 20°C (designated as T_1 for further comparisons). Upon further increasing the temperature, a marked increase in $\nu_s\text{CH}_2$ occurred around $60\text{--}80^\circ\text{C}$, with a midpoint (designated as T_2) near 70°C . Relatively little further increase in $\nu_s\text{CH}_2$ was noted at temperatures above 80°C . The inset in Fig. 2 shows that the variation (estimated by

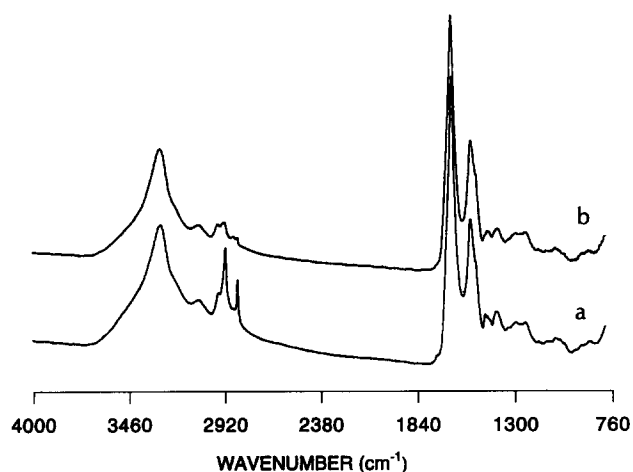


Fig. 1. The representative infrared spectrum of porcine stratum corneum: (a) intact, (b) lipid-depleted.

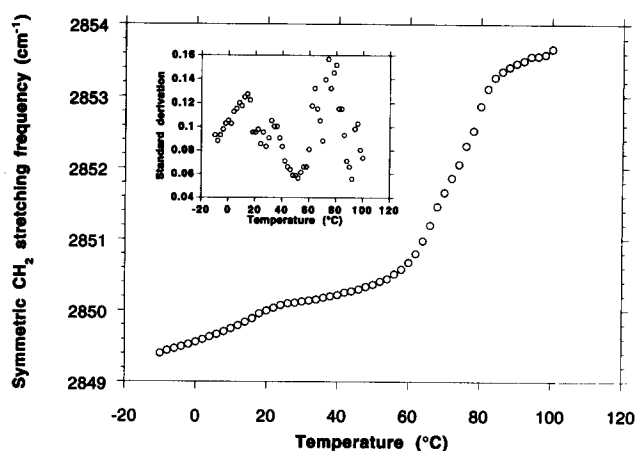


Fig. 2. The temperature-dependence of the symmetric CH_2 stretching frequency from porcine stratum corneum. The inset represents the standard deviation of corresponding data points ($n = 5$).

the standard deviation; $n = 5$) of $\nu_s\text{CH}_2$ was less than 0.2 cm^{-1} at each temperature measured, reflecting the high signal-to-noise ratio of the IR spectra and the precision of the frequency determination, as well as the small variation inherent in these SC samples.

Since the methylene group vibrations from intact SC correspond to the extracellular lipids, an evaluation of the phase behavior of the total lipid extract was of interest. The temperature-induced variation in $\nu_s\text{CH}_2$ for extracted lipids is shown in Fig. 3. The thermal behavior of the extracted lipid was similar to that of the intact sample (Fig. 2). The low- and high-temperature values of $\nu_s\text{CH}_2$ were comparable in both samples, however, the transition T_1 was not apparent and T_2 was lower ($\sim 60^\circ\text{C}$) in isolated SC lipids. In addition, the transition associated with T_2 occurred over a narrower temperature range than that seen in intact samples.

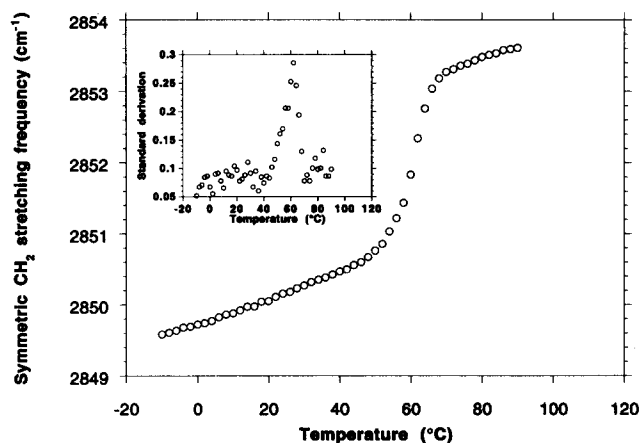


Fig. 3. The temperature-dependence of the symmetric CH_2 stretching frequency from extracted stratum corneum lipids. The inset represents the standard deviation of corresponding data points ($n = 3$).

The CH_2 stretching bandwidth also provides information on the alkyl chain conformation. In particular, band broadening primarily reflects heterogeneity among C-H vibrations due to differences in local conformation and interchain interactions [18]. The temperature-dependent change in the symmetric CH_2 stretching bandwidth for intact SC is shown in Fig. 4. A comparison of $\nu_s\text{CH}_2$ (Fig. 2) and the bandwidth plots shows that while the shape of each was qualitatively similar, the low-temperature inflection ($T_1 \sim 15^\circ\text{C}$) and the midpoint of T_2 ($\sim 60^\circ\text{C}$) occurred at lower temperatures in the bandwidth data. Similar results were obtained for extracted SC lipids (data not shown).

Like the methylene stretching band, the methyl vibrations provide information on the alkyl chain conformation, however, the information is specific for the terminal CH_3 group. The results in Fig. 5 show the asymmetric methyl stretching frequency ($\nu_a\text{CH}_3$) of porcine SC as a function of temperature. These data exhibit a markedly different thermal dependence than the corresponding methylene results ($\nu_s\text{CH}_2$) obtained for the same samples (Fig. 2). In particular, the methyl stretching results show a continuous increase in $\nu_a\text{CH}_3$ over the entire temperature range, with no indication of a phase transition. Similar results were obtained for extracted SC lipids (data not shown).

Noteworthy among these data are the standard deviations of the frequency and bandwidth measurements which show maximal variation at the phase transition temperatures (insets of Figs. 2, 3, 4). We initially speculated this variation to originate from the lateral density fluctuation and domain formation similar to the model proposed by Cruzeiro-Hansson and Mouritsen for lipid phase transition [19]. Nonetheless, the variation also depends on the rate of the temperature-dependent frequency change, thus obscuring the interpretation. In practice, the standard deviation profile serves as a way of verifying the phase transition temperature. Consistent with this note, there was no systematic variation in the standard deviation associated with $\nu_a\text{CH}_3$ (Fig. 5, inset).

Interactions between methylene groups on adjacent alkyl chains affect the CH_2 scissoring and rocking bands which occur near 1470 and 730 cm^{-1} , respectively. A weak shoulder around 1473 cm^{-1} was distinguished in the scissoring band of intact SC, especially at low temperatures (Fig. 6a). Further resolution of the spectrum by deconvolution (Fig. 6b) and second derivative (Fig. 6c) techniques verified the presence of a peak at 1473 cm^{-1} , in addition to revealing two other peaks at 1468 and 1464 cm^{-1} . Based upon reported values of CH_2 scissoring frequency from other alkyl chain systems, the peaks at 1464 and 1473 cm^{-1} are associated with factor group splitting induced by the lateral chain interactions when the carbon skeleton planes of adjacent alkyl chains are perpendicular to each other

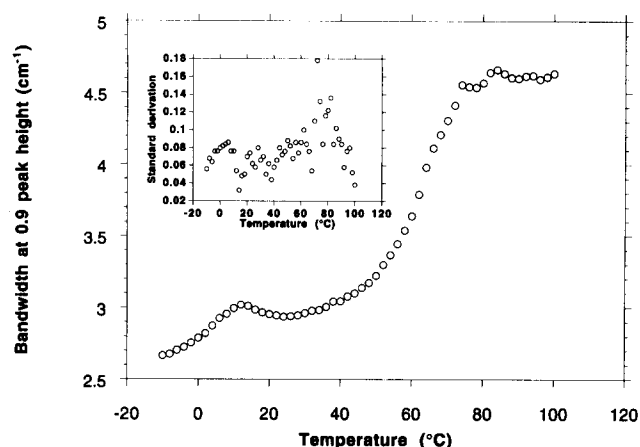


Fig. 4. The temperature-dependence of the symmetric CH_2 stretching bandwidth at 0.9 peak height, from porcine stratum corneum. The inset represents the standard deviation of corresponding data points ($n = 5$).

[20,21]. Factor group splitting was further verified in the SC from the second derivative spectrum of the CH_2 rocking region which exhibited peaks at 729 and 720 cm^{-1} (Fig. 6d). Similar spacing is expected for both the methylene scissoring and the methylene rocking band splittings [22]. The remaining scissoring peak at 1468 cm^{-1} is commonly attributed to the vibration of highly mobile chains packing in a less ordered subcell such as a hexagonal arrangement.

As temperature was increased from -10°C , the whole scissoring band narrowed (data not shown). This corresponded to the diminishing of factor group splitting and the predominance of the 1468 cm^{-1} peak. The presence of factor group splitting (1473 and 1464 cm^{-1}) persists at least up to 40°C , as shown in Fig. 7a where the frequency position of each component in the scissoring band is shown at various temperatures.

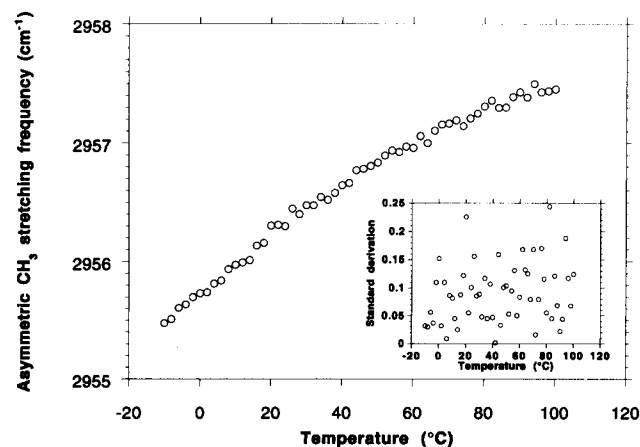


Fig. 5. The temperature-dependence of the asymmetric CH_3 stretching frequency from porcine stratum corneum. To enhance the resolution, the peak was deconvolved using a Bessel apodization function with a half-width of 14 cm^{-1} and a resolution factor of 1.8 before peak picking.

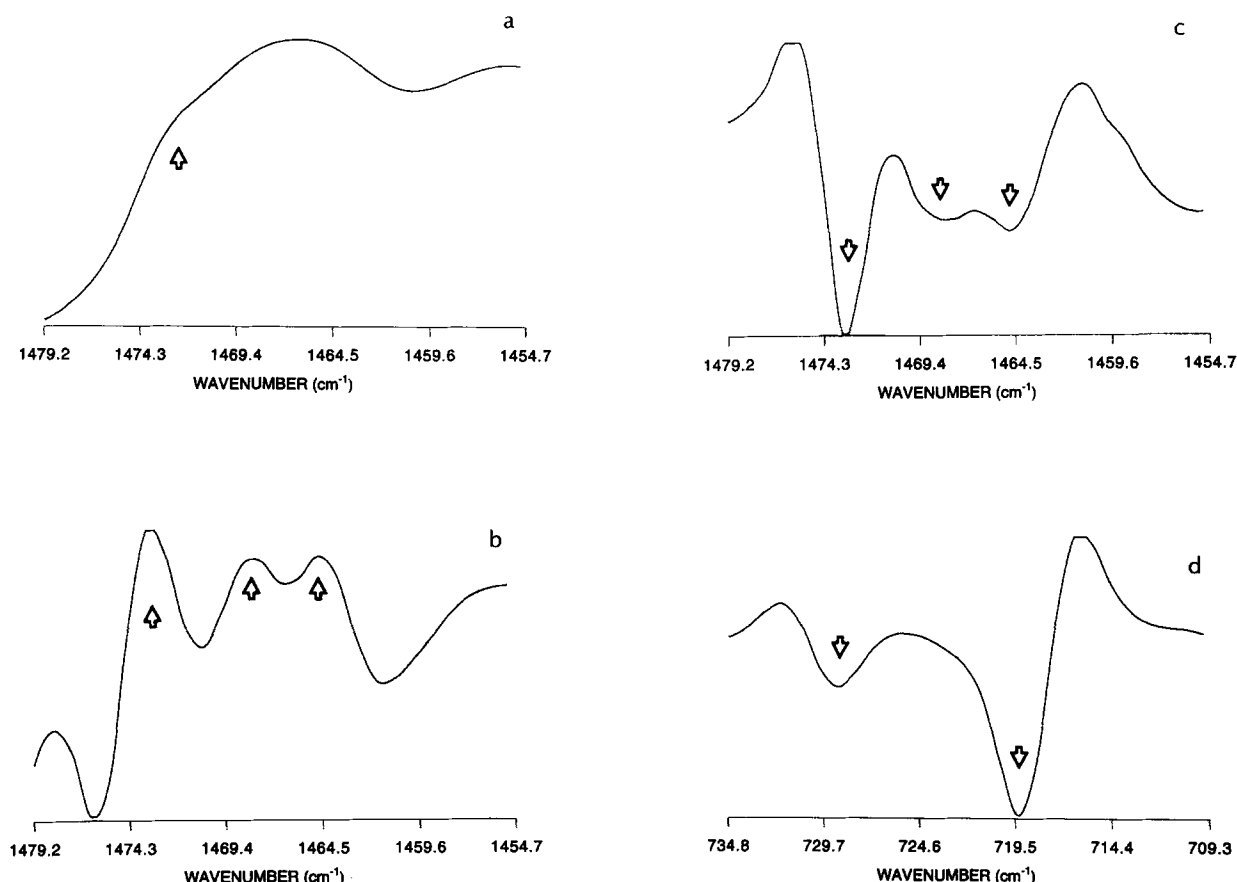


Fig. 6. The CH_2 scissoring and the CH_2 rocking vibrations at -10°C from porcine stratum corneum. (a) The original CH_2 scissoring region. (b) The deconvoluted spectrum of the CH_2 scissoring region. The Bessel apodization function with a half-width of 8 cm^{-1} and a resolution enhancement factor of 2.5 was employed. (c) The second derivative spectrum of the CH_2 scissoring region. (d) The second derivative spectrum of the CH_2 rocking region.

Since the resolution enhancement factor of the deconvolution process should not exceed the logarithm of the signal-to-noise ratio of the original spectrum [23], no attempt was made to increase the resolution factor to precisely determine the disappearance temperature of the splitting. We, however, could estimate the further changes in the factor group splitting by difference spectra. In particular, the spectrum acquired at -10°C was subtracted from the absorbance at -4°C ; the positions of the maximal difference were identified at 1473 and 1463 cm^{-1} , coinciding with the factor group splitting observed by both the deconvoluted and the derivative spectra. Similar subtraction and the positions of maximal differences were also determined at every 6°C increment, i.e., the -4°C data would be subtracted from the 2°C spectrum and so on up to a final temperature of 68°C . Since there was no significant difference among the results obtained below 26°C , Fig. 7b only illustrates the temperature profile of the positions of maximal changes from 26°C to 68°C . The results show that the spacing of factor group splitting diminished with increasing temperature and finally coalesced at about 55 – 60°C . During the gradual disap-

pearance of the splitting, minimal changes in $\nu_s\text{CH}_2$ were observed (Fig. 2).

The investigation of the CH_2 scissoring vibrations from the total lipid extract showed similar observations seen with the intact SC (data not shown). Particularly, the deconvoluted spectrum at -10°C also showed three peaks at 1473 , 1468 and 1464 cm^{-1} . In addition, the CH_2 rocking region of the same sample exhibited a doublet at 729 and 720 cm^{-1} . Finally, the temperature dependence for the lipid extract was identical to that seen in the intact sample (Fig. 7a and b).

4. Discussion

Changes in the frequency and bandwidth of the CH_2 stretching vibrations are directly related to the conformational order of lipid alkyl chains [18]. The symmetric CH_2 stretching vibration is particularly sensitive to the *trans*/*gauche* conformation of the carbon skeleton and, unlike the asymmetric stretching band, it is less susceptible to interference resulting from Fermi resonance interaction [24]. The frequency ($\nu_s\text{CH}_2$) and bandwidth

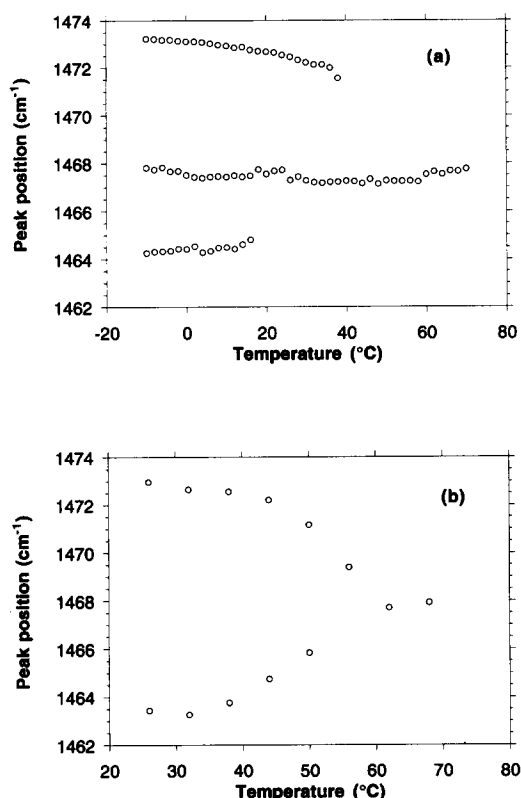


Fig. 7. (a) The temperature-dependence of the CH₂ scissoring band from porcine stratum corneum. Peak positions were determined from the deconvolved spectra. (b) The maximal changes in the difference spectra of the CH₂ scissoring region from the same sample (see text).

of the symmetric CH₂ stretching vibration have been widely used to evaluate the thermal phase behavior of numerous lipid systems. In this study, we evaluated the thermal behavior of SC lipids using these same parameters.

Mammalian SC is an unusual membrane where the lipids are compartmentalized in a continuous extracellular space surrounding discrete cell remnants. Due to the extracellular localization of SC lipids they can be easily extracted with chloroform-methanol [17,25]. Hence, we evaluated the IR spectra of SC samples before and after exhaustive lipid depletion. Those results indicated greater than 90% reduction in the intensity of the methylene stretching bands after lipid extraction. In contrast, no change was noted in the Amide I region (data not shown). Clearly therefore, the CH₂ stretching vibration primarily reflects the properties of the extracellular SC lipids.

Samples of intact SC were heated from -10 to 100°C in the spectrometer. Analysis of temperature-dependent changes in ν_s CH₂ (Fig. 2) showed an increase of about 4 cm⁻¹ over this temperature range, with a particularly abrupt increase from about 60 to 80°C. A similar, temperature-dependent increase in ν_s CH₂ seen

in a variety of other lamellar lipid systems was due to alkyl chain-melting and a resultant increase in the number of *gauche* conformers [18]. The results presented here reflect a similar phase transition, albeit with a transition midpoint near 70°C. Similar results were obtained for SC lipids from various mammals using DSC [4], X-ray diffraction [8,9] and NMR spectroscopy [12].

The lipid nature of this transition was confirmed by IR analysis of solvent extracted material. The temperature-dependent change in ν_s CH₂ for extracted lipids (Fig. 3) shows qualitatively the same behavior as in the intact SC (Fig. 2). A closer comparison of Figs. 2 and 3 indicates several notable differences between the thermal behavior of extracted SC lipids and those in the intact sample. In isolated lipids the alkyl chain-melting transition occurs at a lower temperature, and over a narrower temperature range. These results closely reflect those obtained with DSC where a broad, double-peaked transition near 70°C in intact SC can be compared with a single, narrower transition near 60°C for extracted lipids [4]. The results of Figs. 2 and 3 also show that the inflection in ν_s CH₂ seen at 25°C in the intact sample was not found in extracted lipids. The multiple transitions observed in intact SC are replaced by a single, narrower transition in extracted lipids. Finally, the value of ν_s CH₂ obtained for extracted SC lipids is greater than the corresponding value for intact samples at all temperatures between 36 and 82°C ($P > 0.95$; two-tailed *t*-test) suggesting that greater acyl chain disorder is observed in lipids extracted from the SC.

There are several possible explanations for the low temperature (~20°C) transition seen in the intact SC. It was previously suggested that this transition in human SC reflects surface lipids of sebaceous origin which may coat the sample [11]. The low melting temperature observed here is consistent with the liquid nature of the sebaceous lipids at physiological temperatures. However, porcine SC contains little, if any, sebaceous lipid [25]. A second possibility is that this transition involves a solid-solid phase change. This seems unlikely, however, since the CH₂ scissoring and rocking results (see below) show no transitions at this temperature. A third possible explanation involves a solid to fluid transition of a small fraction of the SC lipids. White et al. [8] have noted from X-ray results that solid and liquid lipids co-exist in mouse SC at temperatures of 25°C and above. In agreement, the value of ν_s CH₂ in SC decreases continuously as the temperature is decreased below 25°C (Fig. 2). Since the all-*trans* configuration is associated with the lowest value of ν_s CH₂, there must be *gauche* conformers at 25°C. Taken together, these results suggest that lipid segregation produces multiple transitions in intact samples, while extracted lipids display a single transition due to mixing.

The bandwidth of the CH_2 stretching peaks reflects chain mobility as well as the distribution and number of alkyl chain conformational states. The results in Fig. 4 show the temperature-dependent increase in bandwidth, with a particularly sharp rise between about 45 and 70°C. A comparison of the results in Figs. 2 and 4 shows that while they are qualitatively similar, the bandwidth transitions occur at lower temperatures. Infrared results obtained with mouse SC also demonstrated that the transition midpoint for the CH_2 stretching bandwidth occurred about 20°C below the value obtained from $\nu_s\text{CH}_2$ data [15]. Similar temperature-dependent behavior of methylene frequency and bandwidth was noted for *Acholeplasma laidlawii* membranes [26] and aqueous surfactant dispersions [27]. Those authors also suggested that the differences reflect the differing sensitivity of each spectral parameter to molecular structure. As noted by Sapper et al. [27] and Dluhy et al. [28], frequency and bandwidth behavior similar to that shown here results from the coexistence of at least two lipid phases of differentially varying absorption bands. Once again, the IR results suggest the coexistence of solid and fluid phases in the SC at temperatures well below the main chain-melting transition. In addition, the expression of lipid phase multiplicity shown by the differences in the frequency and the bandwidth profiles may reflect the double-peaked characteristic of the transition at 60–80°C observed with DSC [4]. This then further suggests that the endothermic transition in the calorimetry scan of SC and the increase in the methylene stretching frequency at 60–80°C originate from the same event, i.e., the melting of lipid alkyl chains which, by deduction from the IR and DSC results, likely consist of two separate populations.

Information on the alkyl chain conformation of the terminal methyl group is provided by $\nu_a\text{CH}_3$. Fig. 5 shows the temperature-dependent change in $\nu_a\text{CH}_3$ for intact SC and indicates no evidence of a phase transition, in sharp contrast to the methylene frequency (Fig. 2) and bandwidth data (Fig. 4). Umemura et al. [29] obtained nearly identical results for DPPC multilayers containing 40 mol% cholesterol, and suggested that the difference between the methyl and methylene behavior was due to increased freedom of motion near the center of the bilayer. The similarity of their results to those shown in Fig. 5, strongly supports the idea that the center of both DPPC and SC lamellae is less constrained than the methylene groups nearer to the polar head group. Thus, like a number of phospholipid bilayers [30,31], SC lipids exhibit a gradient of disorder towards the center of the lamellae.

The CH_2 scissoring and rocking vibrations provide information on alkyl chain packing. In particular, it has been demonstrated that alkyl chains in the ordered, all-*trans* configuration, pack in a solid lattice which

gives rise to factor group splitting of both the CH_2 scissoring and rocking bands [20]. In contrast, the more loosely packed hexagonal phase (sometimes referred to as the rotator phase in alkanes) results in a single peak at a frequency which is intermediate to the factor group splitting. The CH_2 scissoring band of SC exhibited a shoulder near 1473 cm^{-1} at low temperatures. Resolution of the CH_2 scissoring band was enhanced by the use of deconvolution and second derivative techniques, and both the deconvolved (Fig. 6b) and second derivative (Fig. 6c) spectra of intact SC showed peaks at 1473 , 1468 and 1464 cm^{-1} . As demonstrated in numerous phospholipid systems [21,32], the peaks near 1464 and 1473 cm^{-1} are due to orthorhombic gel phase packing, while the single peak near 1468 cm^{-1} is associated with hexagonal packing. Further support of the factor group splitting can be derived from the second derivative spectrum of the CH_2 rocking band which shows peaks near 719 and 729 cm^{-1} (Fig. 6d). In both the scissoring and rocking modes the splitting is near 10 cm^{-1} , indicative of highly ordered alkyl chain packing [21], and consistent with the long, saturated alkyl chains which predominate in SC lipids [25].

The temperature dependent changes in the CH_2 scissoring band are shown in Fig. 7a and b. The results in Fig. 7a show that from -10 to about 40°C three peaks were seen, consistent with the coexistence of orthorhombic and hexagonal packing. From the difference spectra (Fig. 7b), it is clear that orthorhombic packing persists to about 55 – 60°C . Thus, these results indicate that at temperatures up to just below the chain-melting transition, orthorhombic and hexagonal solid phases coexist. In addition, recent X-ray diffraction results have shown the coexistence of orthorhombic and hexagonal phases in human and mouse SC [9,10]. In contrast, these investigators found no orthorhombic reflections in porcine SC hydrated at 60% relative humidity (Bouwstra, personal communication). The IR data presented here suggest the coexistence of a highly ordered orthorhombic phase along with a separate, more loosely ordered hexagonal phase in porcine SC lipids at temperatures below the alkyl chain-melting transition.

Umemura et al. [29] studied the gel phase behavior of DPPC multilayers in the presence and absence of cholesterol. Their CH_2 scissoring and rocking results obtained with pure DPPC showed factor group splitting which collapsed to a single peak, at intermediate frequency, at about 36°C . These results were associated with an orthorhombic to hexagonal transition in the gel state (the so-called pre-transition) which occurred at about 5°C below the chain-melting transition. Results obtained with DPPC plus 40 mol% cholesterol, however, showed the coexistence, at temperatures below 30°C , of peaks due to both orthorhombic and hexagonal phases. Further, since factor group splitting re-

quires an ordered, all-*trans* configuration, and since cholesterol induces a greater *gauche* population, they concluded that the orthorhombic phase contained pure DPPC, while the hexagonal phase contained cholesterol and DPPC.

The CH₂ scissoring results obtained by Umemura et al. [29] for DPPC plus cholesterol are qualitatively and quantitatively similar to those presented in Fig. 7a and b, suggesting that the coexistence of orthorhombic and hexagonal phases also occurs in SC lipids (which contain a similar amount of cholesterol). Based on the striking similarity of our results to those of Umemura et al. [29], it is reasonable to propose that in SC lipids the hexagonal phase contains cholesterol and *gauche* alkyl conformers, while the orthorhombic phase contains no cholesterol and alkyl chains in the predominantly all-*trans* configuration. Consistent with this hypothesis are the calorimetry results of Wiedmann and Salman [33] obtained with hydroxyceramide and cholesterol. Their results suggested that the addition of 40 to 50 mol% cholesterol to a mixture of hydroxyceramides resulted in the coexistence of two phases, one containing cholesterol plus ceramides, and the second containing only ceramides. Taken together, then, these results suggest the existence of a highly ordered orthorhombic phase, and a more loosely ordered hexagonal phase in SC lipids at physiological temperatures. Moreover, since cholesterol is known to induce greater *gauche* conformers at temperatures below the chain-melting transition, it seems likely that cholesterol is associated with the hexagonal phase. In contrast, the orthorhombic phase most likely comprises long, saturated alkyl chains, characteristic of SC ceramides and fatty acids [25].

In summary, evidence and arguments which support the lipid segregation as the basis for multiple phase transitions observed with either FTIR or DSC in SC lipids are reported here. The results presented here for SC lipids also show surprising similarities to results obtained for phospholipid systems. In particular, the results show that SC lipids undergo a phase transition associated with alkyl chain-melting, and that there is a gradient of disorder along the alkyl chain. Furthermore, like high cholesterol content phospholipid bilayers, the SC lipids are characterized by the coexistence of ordered and disordered phases at temperatures below the chain-melting transition. These similarities are particularly interesting given the profound differences in composition and lamellar structure between phospholipids and SC lipids.

5. Acknowledgement

B.O. is grateful for the support she received from Professor Ronald R. Burnette at the School of Phar-

macy, University of Wisconsin, during the course of this work through the graduate student program.

6. References

- [1] Scheuplein, R.J. and Blank, I.H. (1971) *Physiol. Rev.* 51, 702–747.
- [2] Potts, R.O. and Guy, R.H. (1992) *Pharm. Res.* 9, 663–669.
- [3] Potts, R.O. and Francoeur, M.L. (1990) *Proc. Natl. Acad. Sci. USA* 87, 3871–3873.
- [4] Golden, G.M., Guzek, D.B., Kennedy, A.H., McKie, J.E. and Potts, R.O. (1987) *Biochemistry* 26, 2382–2388.
- [5] Wertz, P.W. and Downing, D.T. (1983) *J. Lipid Res.* 24, 759–765.
- [6] Elias, P.M. and Friend, D.S. (1975) *J. Cell. Biol.* 65, 180–191.
- [7] Madison, K.C., Swartzendruber, D.C., Wertz, P.W. and Downing, D.T. (1987) *J. Invest. Dermatol.* 88, 714–718.
- [8] White, S.H., Mirejovsky, D. and King, G.L. (1988) *Biochemistry* 27, 3725–3732.
- [9] Bouwstra, J.A., Gooris, G.S., Van der Spek, J.A. and Bras, W. (1991) *J. Invest. Dermatol.* 97, 1005–1012.
- [10] Bouwstra, J.A., Gooris, G.S., Salomons-de Vries, M.A., Van der Spek, J.A. and Bras, W. (1992) *Int. J. Pharm.* 84, 205–216.
- [11] Golden, G.M., Guzek, D.B., Harris, R.R., McKie, J.E. and Potts, R.O. (1986) *J. Invest. Dermatol.* 86, 255–259.
- [12] Abraham, W. and Downing, D.T. (1991) *Biochim. Biophys. Acta* 1068, 189–194.
- [13] Thewalt, J., Kitson, N., Arajo, C., MacKay, A. and Bloom, M. (1992) *Biochem. Biophys. Res. Commun.* 188, 1247–1252.
- [14] Thewalt, J., Bloom, M. and Kitson, N. (1992) *J. Invest. Dermatol.* 98, 642.
- [15] Knutson, K., Krill, S.L., Lambert, W.J. and Higuchi, W.I. (1987) *J. Controlled Release* 6, 59–74.
- [16] Wertz, P.W. and Downing, D.T. (1989) in *Transdermal Drug Delivery. Developmental Issues and Research Initiatives*, pp. 10.
- [17] Wertz, P.W. and Downing, D.T. (1987) *Biochim. Biophys. Acta* 917, 108–111.
- [18] Mantsch, H.H. and McElhaney, R.N. (1991) *Chem. Phys. Lipids* 57, 213–226.
- [19] Cruzeiro-Hansson, L. and Mouritsen, O.G. (1988) *Biochim. Biophys. Acta* 944, 63–72.
- [20] Snyder, R.G. (1979) *J. Chem. Phys.* 71, 3229–3235.
- [21] Cameron, D.G., Gudgin, E.F. and Mantsch, H.H. (1981) *Biochemistry* 20, 4496–4500.
- [22] Koyama, Y., Yanagishita, M., Toda, S. and Matsuo, T. (1977) *J. Colloid Interface Sci.* 61, 438–445.
- [23] Mantsch, H.H., Moffatt, D.J. and Casal, H.L. (1988) *J. Mol. Struct.* 173, 285–298.
- [24] Snyder, R.G., Hsu, S.L. and Krimm, S. (1978) *Spectrochim. Acta* 34A, 395–406.
- [25] Downing, D.T. (1992) *J. Lipid Res.* 33, 301–313.
- [26] Casal, H.L., Cameron, D.G., Smith, I.C.P. and Mantsch, H.H. (1980) *Biochemistry* 19, 444–451.
- [27] Sapper, H., Cameron, D.G. and Mantsch, H.H. (1981) *Can. J. Chem.* 59, 2543–2549.
- [28] Dluhy, R.A., Chowdhry, B.Z. and Cameron, D.G. (1985) *Biochim. Biophys. Acta* 821, 437–444.
- [29] Umemura, J., Cameron, D.G. and Mantsch, H.H. (1980) *Biochim. Biophys. Acta* 602, 32–44.
- [30] Vincent, M. and Gallay, J. (1984) *Biochemistry* 23, 6514–6522.
- [31] Thulborn, K.R., Tilley, L.M., Sawyer, W.H. and Treloar, E. (1979) *Biochim. Biophys. Acta* 558, 166–178.
- [32] Cameron, D.G., Casal, H.L. and Mantsch, H.H. (1980) *Biochemistry* 19, 3665–3672.
- [33] Wiedmann, T.S. and Salmon, A. (1991) *Lipids* 26, 364–368.